



LIVER CANCER

Anti-hepatoma activity and mechanism of ursolic acid and its derivatives isolated from *Aralia decaisneana*

Ze Tian, Geng Lin, Rui-Xia Zheng, Feng Huang, Meng-Su Yang, Pei-Gen Xiao

Ze Tian, Geng Lin, Rui-Xia Zheng, Feng Huang, Pei-Gen Xiao, Department of Pharmacology, Institute of Medicinal Plant Development, Chinese Academy of Medical Sciences, Peking Union Medical College, Beijing 100094, China
Meng-Su Yang, Department of Biology and Chemistry, City University of Hong Kong, Kowloon, Hong Kong, China
Supported by the National Natural Science Foundation of China, No. 30470195

Co-correspondence: Pei-Gen Xiao

Correspondence to: Ze Tian, Associate Professor of Institute of Medicinal Plant Development, Chinese Academy of Medical Sciences, Peking Union Medical College, Beijing 100094, China. ztian603@hotmail.com

Telephone: +86-10-62894597 Fax: +86-10-62894597

Received: 2005-07-17 Accepted: 2005-07-29

Tian Z, Lin G, Zheng RX, Huang F, Yang MS, Xiao PG. Anti-hepatoma activity and mechanism of ursolic acid and its derivatives isolated from *Aralia decaisneana*. *World J Gastroenterol* 2006; 12(6): 874-879

<http://www.wjgnet.com/1007-9327/12/874.asp>

Abstract

AIM: To investigate the anti-tumor activity of ursolic acid (UA) and its derivatives isolated from *Aralia decaisneana* on hepatocellular carcinoma both *in vitro* and *in vivo*.

METHODS: *In vivo* cytotoxicity was first screened by 3-[4,5-dimethylthiazol-2-yl]-2, 5-diphenyltetrazolium bromide (MTT) assay. Morphological observation, DNA ladder, flow cytometry analysis, Western blot and real time PCR were employed to elucidate the cytotoxic mechanism of UA. Implanted mouse hepatoma H₂₂ was used to evaluate the growth inhibitory effect of UA *in vivo*.

RESULTS: UA could significantly inhibit the proliferation of HepG2 and its drug-resistance strain, R-HepG2 cells, but had no inhibitory effect on primarily cultured normal mouse hepatocytes whereas all the six derivatives of UA could not inhibit the growth of all tested cell lines. Further study on mechanism demonstrated that apoptosis and G₀/G₁ arrest were involved in the cytotoxicity and cleavage of poly-(ADP-ribose)-polymerase (PARP). Downregulation of cyclooxygenase-2 (COX-2) protein and upregulation of heat shock protein (HSP) 105 mRNA correlated to the apoptosis of HepG2 cells treated with UA. In addition, UA also could inhibit the growth of H₂₂ hepatoma *in vivo*.

CONCLUSION: UA is a promising anti-tumor agent, but further work needs to be done to improve its solubility.

© 2006 The WJG Press. All rights reserved.

Key words: *Aralia decaisneana*; Ursolic acid; Hepatoma

INTRODUCTION

Hepatocellular carcinoma is one of the most common malignant neoplasms worldwide and one of the leading causes of malignancy-related death in China^[1,2]. Its therapy in clinic is still a big challenge.

Ursolic acid (UA) is a versatile compound, which possesses anti-cancer^[3,4], anti-inflammatory^[5,6], anti-HIV^[7] and immunomodulatory effects^[8]. There is a growing interest in the anti-tumor activities of UA. UA could act on almost all steps in the whole cancer process: initiation, promotion, progression, and metastasis. Multiple lines of evidence indicate that UA is a promising chemo-preventive agent both *in vivo* and *in vitro*. UA could inhibit Epstein-Barr virus activation induced by 12-*O*-tetradecanoylphorbol-13-acetate in Raji cells and two-stage mouse skin tumor promotion^[9,10]. The mechanism involved might associate with the inhibition of AP-1-mediated induction of COX-2 by disrupting PKC signal transduction pathway^[11]. UA could inhibit the proliferation of various cancerous cell lines by inhibiting DNA polymerase and topoisomerase^[12], inducing apoptosis through proteolytic activation of caspase-3 and/or other similar caspases^[3]. It was also reported that UA has anti-invasion and anti-metastasis activity by inhibiting nuclear factor-kappa B (NF- κ B) activation, down-regulating COX-2 and matrix metalloproteinase 9^[13].

Besides its cytotoxicity to hepatoma, it was reported that UA can exert its hepatoprotective action in mice and rats^[14-16]. The reason for the phenomenon is worth studying. Moreover, the growth inhibitory activity of UA on hepatocellular carcinoma *in vivo* is still unknown.

In the present study, UA and its six derivatives isolated from the bark of *Aralia decaisneana* were used to treat rheumatism, lumbago, hepatitis, nephritis, and diabetes mellitus in Chinese folk medicine. The cytotoxicity of these UA compounds to HepG2, its drug-resistance strain R-HepG2 and primarily cultured normal mouse and rat hepatocytes were examined in order to find their anti-hepatoma efficiency on both parental and drug-resistant hepatocellular carcinoma as well as their low toxicity.

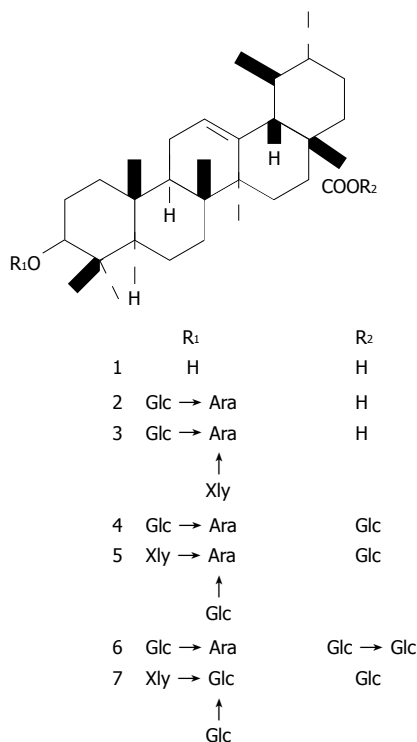


Figure 1 Structures of UA and its derivatives.

1. UA
2. UA-3-O-β-D-glucopyranosyl-(1→3)-α-L-arabinopyranoside,
3. UA-3-O-[[β-D-xylopyranosyl-(1→2)]]β-D-glucopyranosyl-(1→3)]-α-L-arabinopyranoside,
4. UA-3-O-β-D-glucopyranosyl-(1→3)-α-L-arabinopyranosyl-28-O-β-D-glucopyranoside,
5. UA-3-O-[[β-D-glucopyranosyl-(1→2)]]β-D-xylopyranosyl-(1→3)]-α-L-arabinopyranosyl-28-O-β-D-glucopyranoside,
6. UA-3-O-β-D-glucopyranosyl-(1→3)-α-L-arabinopyranosyl-28-O-β-D-glucopyranosyl-(1→6)-O-β-D-glucopyranoside,
7. UA-3-O-[[β-D-glucopyranosyl-(1→2)]]β-D-xylopyranosyl-(1→3)]-β-D-xylopyranosyl-28-O-β-D-glucopyranoside.

Morphological observation, DNA ladder, cell cycle analysis, Western blot and real time PCR were performed to elucidate the cytotoxic mechanism of UA on HepG2 cells. Mice bearing murine hepatoma H₂₂ were used to investigate the growth inhibitory effect of UA *in vivo*.

MATERIALS AND METHODS

Tissue culture and drug treatment

HepG2 (ATCC) cells were maintained in RPMI 1640 (Gibco) containing 10% FBS (Gibco), 2 mg/mL sodium bicarbonate, 100 µg/mL penicillin sodium salt and 100 µg/mL streptomycin sulfate. R-HepG2 (City University of Hong Kong) was maintained in the presence of 1.2 µmol/L doxorubicin (Sigma). Hepatocytes were isolated from normal Kunming mice (Experimental Animal Centre of Zhongshan Medical University) and SD rats (Experimental Animal Centre of Zoology, Chinese Academy of Sciences) with enzymatic perfusion technique as previously described^[17]. Logarithmically growing cells were used for all the experiments.

UA and its derivatives (Figure 1) were isolated from the bark of *Aralia decaisneana* by silica gel column chromatography and their structures were identified by spectral analysis^[18]. UA was dissolved in DMSO at the

concentration of 100 and 10 mmol/L in cellular and *in vivo* experiments, respectively and diluted in tissue culture medium and saline before use. Six UA derivatives were directly dissolved in tissue culture medium.

Cytotoxicity assay

HepG2 and R-HepG2 cells (1.5×10^4) as well as mouse and rat hepatocytes (8×10^3) were seeded in 96-well plates and treated with the compounds at various concentrations (3.125–100 µmol/L). Then the cells were incubated at 37 °C in an atmosphere containing 50 mL/L CO₂ for 48 h followed by MTT assay. IC₅₀ of the tested compounds on different cell lines were obtained from the concentration–effect curves.

Morphology observation

HepG2 cells were cultured in 3.5-cm dishes. UA was added to the medium at 20 µmol/L for 6, 12, and 24 h. A harringtonin-(20 µmol/L, 24 h) and vehicle-(0.1% DMSO) treated sample was regarded as a positive and negative control, respectively. After the treatment, all the cultures were incubated at 37 °C in an atmosphere containing 50 mL/L CO₂ for the indicated time. Photographs were taken under an inverted Leica fluorescence 40×10 microscope after acridine orange (AO)/ethidium bromide (EB) staining.

DNA ladder analysis

HepG2 cells were grown to 70–80% confluence and exposed to 20 µmol/L UA or harringtonin. Then the cultures were incubated at 37 °C in an atmosphere containing 50 mL/L CO₂ and collected at 0, 6, 12, and 24 h. Their genomic DNA was extracted and analyzed by gel electrophoresis^[19].

Flow cytometry analysis

Flow cytometry analysis was used to evaluate cell cycle distribution of HepG2 cells. HepG2 cells were treated with 20 µmol/L UA for 0, 6, 12, and 24 h, respectively, collected and fixed in 70% cold ethanol (–20 °C) overnight. After being washed twice with PBS, the cells were resuspended in PBS. RNA in the fixed cells was digested using RNase A (0.5 mg/mL) at 37 °C for 1 h. Finally, the cells were stained with 2.5 µg/mL propidium iodide (PI). The DNA content of the cells was then analyzed with an FACSCalibur instrument (Becton-Dickinson) at excitation 488/emission 600 nm. Data were analyzed by cell cycle distribution software (ModFit LT version 2.0, Verity Software House, USA).

Western blotting

After the treatment, cells were washed thrice with ice-cold PBS and collected with lysis buffer. Protein determination, SDS-PAGE and transfer were performed as previously described^[17]. Nitrocellulose membranes were then incubated with a monoclonal anti-PARP or polyclonal anti-COX-2 antiserum. Secondary antibody to IgG conjugated to horseradish peroxidase was used. The blots were probed with the ECL Western blot detection system according to the manufacturer's instructions.

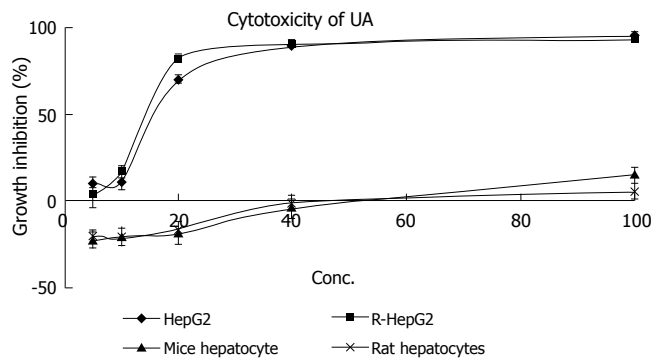


Figure 2 Cytotoxicity of UA to a panel of hepatocytes.

RT-PCR and real time PCR analysis

Total RNA was isolated from HepG2 cells using Trizol reagent according to the standard protocol and used to generate cDNA in each sample using the SuperScript II reverse transcriptase with oligo (dT) primers. Aliquots of total cDNA were diluted and added into each PCR reaction mixture together with 0.5 μmol/L of forward and reverse primers of HSP 105 (F: CAGGATCCAGTTGTACGTGCTC; R: TGATGTGGAGGTTTCAGCACC, 197 bp) and glyceraldehyde-3-phosphate dehydrogenase (GAPDH, F: ATCAGCAATGCCTCCTGCA; R: CCTGCTTCACCACCTTCTTGA, 355 bp) (Shanghai Biotech Engineering Service Limited Company). PCR amplification was performed on a GeneAmp 9700 PCR System (ABI). After denaturation of cDNA at 94 °C for 3 min, the cycling conditions were as follows: 32 cycles consisting of denaturation at 94 °C for 30 s, annealing at 59 °C for 30 s, and extension at 72 °C for 1 min. The PCR products were analyzed by agarose gel electrophoresis and Bio-Rad Chemi Doc. The mRNA expression levels were normalized to the expression of a housekeeping gene GAPDH. SYBR-Green-I fluorescence labeling method was used in real-time quantitative RT-PCR amplification on an ABI Prism 7000 SDS and analyzed with its software according to the standard protocol and manufacturer's instructions^[20]. The $2^{-\Delta\Delta CT}$ method was used in data analysis based on similar (<10%) amplification efficiency of the target and reference genes, which was achieved by the determination of ΔCT variations with template dilution^[21]. GAPDH was used as a reference gene for internal control.

Anti-tumor evaluation on implanted mouse H₂₂

Male CD-1 (ICR) mice (Beijing Vital Laboratory Animal Technology Company) weighing 20–22 g were used for the implantation of hepatoma H₂₂ (s.c.) which was maintained by weekly i.p. passages in CD-1 (ICR) mice, 0.2 mL ascites of 1:6 dilution from tumor-bearing mice 7 days after the tumor inoculation was implanted (s.c.) into the armpit region of the mice. Eight mice were treated i.p. with either UA or vehicle (1% DMSO in saline) once a day for 10 days 24 h after the tumor inoculation. Cyclophosphamide (10 mg/kg b.w.) was used as positive control. Tumor inhibition rate (TIR) was derived from $(1-T/C) \times 100$, where T is the mean tumor weight of the UA-treated group and C is the mean tumor weight of the negative control group.

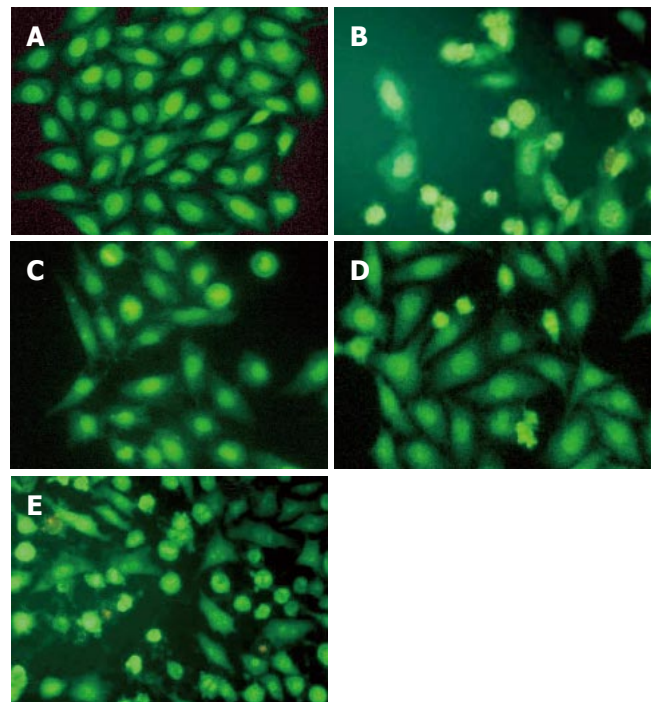


Figure 3 Morphological changes of HepG2 cells in response to harringtonin and UA. Cells were stained with AO/EB and observed under an inverted Leica fluorescence 40×10 microscope. A: Normal HepG2 cells; B: harringtonin (20 μmol/L) for 24 h; C-E: UA (20 μmol/L) for 6, 12, and 24 h, respectively.

Statistical analysis

Student's *t*-test was used in all the experiments. $P < 0.05$ was considered statistically significant.

RESULTS

Selective cytotoxicity

Cytotoxicity of UA and its derivatives was determined by MTT assay. UA was demonstrated to have similar anti-proliferation activity on HepG2 and R-HepG2 cells in a concentration-dependent manner (Figure 2) with its IC₅₀ value being 18 and 15 μmol/L, respectively, whereas it exhibited less growth inhibitory activity on primarily cultured normal mouse and rat hepatocytes and the IC₅₀ value could not be detected at the tested concentration. On the contrary, six UA derivatives did not show any cytotoxicity to all the tested cells, while they possessed better solubility in water than UA.

Morphological changes of HepG2 cells

HepG2 cells treated with harringtonin and 20 μmol/L UA showed similar and significant changes (Figure 3). Chromatin aggregation, nuclear, and cytoplasmic condensation only could be seen in a few cells after being treated with UA for 6 and 12 h. Partition of cytoplasm and nuclei into the membrane bound-vesicles (apoptotic bodies) was observed in the cells treated with harringtonin and UA for 24 h. At the same time, apoptotic cells were found at this time point.

DNA ladder analysis of HepG2 cells

DNA ladder was used to prove the apoptosis of HepG2 cells induced by UA. After treatment with 20 μmol/L

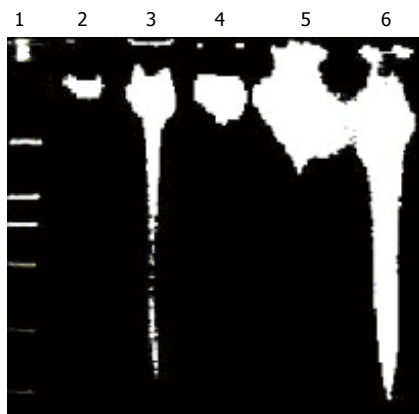


Figure 4 Induction of time-dependent fragmentation of nuclear DNA by harringtonin and UA. Genomic DNA of the treated cells was collected at different time points during the incubation. Lane 1: DNA marker (DL-2000); lane 3: harringtonin (20 $\mu\text{mol/L}$) for 24 h; lanes 2, 4–6: UA (20 $\mu\text{mol/L}$) for 0, 6, 12, and 24 h, respectively.

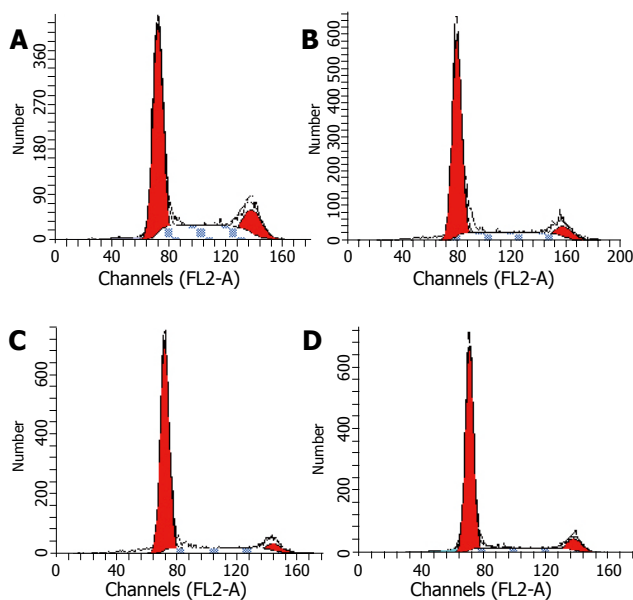


Figure 5 Cell cycle analysis of HepG2 cells treated with UA (20 $\mu\text{mol/L}$) for 0 (A), 6 (B), 12 (C), and 24 h (D), respectively. Cells were stained with PI and analyzed by flow cytometry.

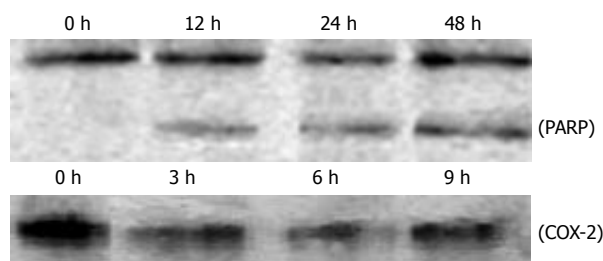


Figure 6 Cleavage of PARP and downregulation of COX-2 protein expression in HepG2 cells treated with UA. Cellular lysate protein (23 $\mu\text{g/lane}$) was loaded for 10% SDS-polyacrylamide gel electrophoresis, and subsequently transferred onto nitrocellulose. Immunoblots were probed with antibody specific for PARP and COX-2 protein. Lysates were from HepG2 cells treated with 20 $\mu\text{mol/L}$ UA for indicated times.

UA for different time points, evident DNA ladder was detected at 24 h on HepG2 cells treated with UA and

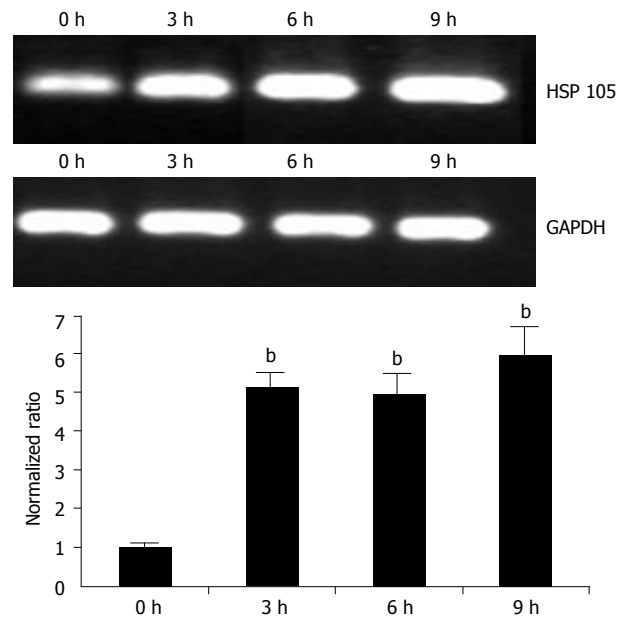


Figure 7 RT-PCR and real time PCR analysis of up-regulated HSP 105 gene in HepG2 cells in response to treatment with UA. HepG2 cells were treated with 20 $\mu\text{mol/L}$ UA for 0, 3, 6, and 9 h. Total RNA was isolated and subjected to semi-quantitative and quantitative RT-PCR analysis. GAPDH was used as a control. For quantitative analysis, data shown are mean \pm SD. $^bP < 0.001$ vs control, $n = 3$.

harringtonin (Figure 4), indicating the apoptosis observed in morphological inspection.

Cell cycle distributions in HepG2 cells

After being exposed to 20 $\mu\text{mol/L}$ UA for 0, 6, 12, and 24 h, respectively, the cell cycle progression of HepG2 cells showed evident changes (Figure 5). UA caused significant G_0/G_1 arrest with a concomitant decrease of cell population in S and G_2/M phases. The distribution of cell cycle in G_0/G_1 , S and G_2/M phases was 57.80%, 27.24%, and 14.96% at 0 h; 67.78%, 22.92%, and 9.3% at 6 h; 73.73%, 19.59%, and 6.69% at 12 h; 74.31%, 15.69%, and 10.0% at 24 h, respectively. When treated with UA for 12 and 24 h, higher percentage of cell cycle distribution in G_0/G_1 phase was detected than that at 6 h.

Cleavage of PARP protein and downregulation of COX-2

Exposure to 20 $\mu\text{mol/L}$ UA for 0, 12, 24, and 48 h, respectively, PARP was cleaved into 89- and 24-kDa fragments, indicating that the apoptosis of HepG2 cells induced by UA was involved in caspase activation. After HepG2 cells were treated with UA for 0, 3, 6, and 9 h, respectively, COX-2 expression was significantly inhibited (Figure 6).

Upregulation of HSP 105 mRNA expression

HSP 105 belongs to HSP 70 super family and is closely related with apoptosis. The amplification efficiency of target and reference genes HSP 105 and GAPDH was quite similar (data not shown). The $2^{-\Delta\Delta C_t}$ method was used in data analysis. After being treated with 20 $\mu\text{mol/L}$ UA for 3, 6, and 9 h, respectively, HSP 105 mRNA expression was upregulated in a time-dependent manner both in RT-PCR and real time PCR (Figure 7).

Table 1 Tumor growth inhibition effect of UA in mice bearing H₂₂ (mean±SD, *n* = 8)

Samples	Dosage (mg/kg)	Tumor weight (g)	Growth inhibition (%)
Control		2.8±1.22	
C.P.	10	1.07±0.55 ^b	61.1
UA	30	1.27±0.90 ^a	54.6
UA	15	1.55±0.91 ^a	44.6

^a*P*<0.05, ^b*P*<0.01 vs control.

Tumor growth inhibitory effect

Twenty-four hours after tumor implantation, administration of UA (30 and 15 mg/kg b.w.) and cyclophosphamide (10 mg/kg b.w.) once a day for 10 days, could significantly suppress the growth of H₂₂ (Table 1). Significant body weight loss was observed in cyclophosphamide-treated group compared to the control group, whereas only slight body weight loss was observed in UA-treated group, suggesting that UA might possess anti-hepatoma effect *in vivo* with low toxicity.

DISCUSSION

In terms of cancer treatment, chemotherapy has serious limitations, namely the lack of selectivity of active ingredients and resistance of cancer cells to these chemicals^[22]. Thus, it is urgent to find new compounds that can kill both parental cancer cells and drug resistant cells and differentiate between normal and cancer cells in order to selectively kill cancerous cells with reduced toxicity. UA possesses good cytotoxicity on HepG2 and R-HepG2 cells, but no cytotoxicity to primarily cultured normal mouse and rat hepatocytes has been detected at corresponding concentrations. These results indicate that UA is a promising anti-tumor agent to parental and drug resistant HepG2 cells with low toxicity and could partially explain why UA inhibits the proliferation of hepatoma while possesses hepatoprotective activity. In addition, UA can lead to apoptosis, DNA ladder and PARP protein cleavage as well as G₀/G₁ cell-cycle arrest.

However, the cytotoxic mechanisms of HepG2 cells induced by UA are not completely understood. PARP is a substrate of apoptosis specific protease from the ICE-family (caspases). The 113 ku PARP is cleaved during apoptosis into 89- and 24-ku fragments which could serve as an early hallmark of apoptosis. In our study, cleaved PARP protein not only further proved apoptosis, but also it was implied that activation of caspases was involved in apoptosis of HepG2 cells treated with UA. COX-2 is an early-response gene that is highly inducible by mitogenic and inflammatory stimuli^[23-25]. Multiple lines of evidence suggest that COX-2 is important in carcinogenesis and overexpressed in cancer cells^[26,27]. NS-398, a representative of non-selective COX inhibitors can induce G₀/G₁ cell cycle arrest through inhibition of CDK2 and induction of p21 and p27^[28,29]. Upregulation of p21 could further stimulate mRNA transcription of cytochrome C and caspase 3 which induces apoptosis in the end^[30]. In the light of our study, UA could significantly inhibit COX-2 protein expression, suggesting that inhibition of

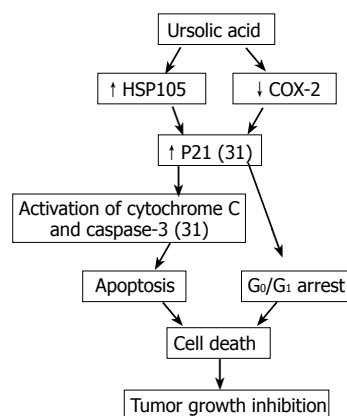


Figure 8 Summary of current understanding of cytotoxicity of UA to hepatoma cells. Functions with reference number represent known mechanism and bold words without reference number represent the mechanism revealed in our study.

COX-2 may correlate with increased p21 expression and subsequent activation of cytochrome C and caspase-3 in HepG2 cells treated with UA^[31].

HSP 105 belonging to heat shock protein (HSP) 70 super family acts as a chaperone and plays a role in control of cell proliferation and cellular aging. It was reported that overexpression of HSP105α could enhance stress-induced apoptosis, but not necrosis in mouse embryonal F9 cells^[32,33]. Some HSPs purified from murine tumors and used as vaccine are prophylactically and therapeutically effective in cancer immunotherapy models^[34]. Further more, MKT-077, a cationic rhodacyanine dye analog exerts its selective toxicity to cancer cells by binding to the HSP 70 family protein mot-2 and reactivating p53 function, thus resulting in increased p53 downstream gene p21 expression^[35]. Upregulation of HSP 105 and increase of p21 expression^[31] may contribute to apoptosis and G₀/G₁ cell-cycle arrest induced by UA, which are at least partially responsible for the selectivity of UA for cancer cells.

Tumor growth inhibitory effect in mice bearing hepatoma could predict the activity of corresponding tumors in human beings. Accordingly, the anti-neoplasm action of UA on mouse hepatoma H₂₂ indicates that it can be used to treat human hepatoma. However, few researches have been done on the pharmacokinetics of UA. We also did not monitor the concentration of UA in the blood of mice. Therefore, more attention should be paid to the active plasma concentration of UA in future.

In conclusion, UA is a potential anti-hepatoma agent with reduced toxicity both *in vitro* and *in vivo*. Summary of current understanding of anti-tumor activity of UA on hepatoma is shown in Figure 8. However, poor water solubility of UA has confined its use. Although its derivatives have good water solubility, these derivatives possess no anti-neoplasm activity. More work should be done to solve this problem.

REFERENCES

- Zhu ZZ, Cong WM, Liu SF, Dong H, Zhu GS, Wu MC. Homozygosity for Pro of p53 Arg72Pro as a potential risk factor for hepatocellular carcinoma in Chinese population. *World J Gastroenterol* 2005; **11**: 289-292

- 2 **Yuan SL**, Wei YQ, Wang XJ, Xiao F, Li SF, Zhang J. Growth inhibition and apoptosis induction of tanshinone II-A on human hepatocellular carcinoma cells. *World J Gastroenterol* 2004; **10**: 2024-2028
- 3 **Hollosy F**, Meszaros G, Bokonyi G, Idei M, Seprodi A, Szende B, Keri G. Cytostatic, cytotoxic and protein tyrosine kinase inhibitory activity of ursolic acid in A431 human tumor cells. *Anticancer Res* 2000; **20**: 4563-4570
- 4 **Hsu HY**, Yang JJ, Lin CC. Effects of oleanolic acid and ursolic acid on inhibiting tumor growth and enhancing the recovery of hematopoietic system postirradiation in mice. *Cancer Lett* 1997; **111**: 7-13
- 5 **Diaz AM**, Abad MJ, Fernandez L, Recuero C, Villaescusa L, Silvan AM, Bermejo P. In vitro anti-inflammatory activity of iridoids and triterpenoid compounds isolated from *Phillyrea latifolia* L. *Biol Pharm Bull* 2000; **23**: 1307-1313
- 6 **Baricevic D**, Sosa S, Della Loggia R, Tubaro A, Simonovska B, Krasna A, Zupancic A. Topical anti-inflammatory activity of *Salvia officinalis* L. leaves: the relevance of ursolic acid. *J Ethnopharmacol* 2001; **75**: 125-132
- 7 **Min BS**, Jung HJ, Lee JS, Kim YH, Bok SH, Ma CM, Nakamura N, Hattori M, Bae K. Inhibitory effect of triterpenes from *Crataegus pinatifida* on HIV-I protease. *Planta Med* 1999; **65**: 374-375
- 8 **Raphael TJ**, Kuttan G. Effect of naturally occurring triterpenoids glycyrrhizic acid, ursolic acid, oleanolic acid and nomilin on the immune system. *Phytomedicine* 2003; **10**: 483-489
- 9 **Banno N**, Akihisa T, Tokuda H, Yasukawa K, Higashihara H, Ukiya M, Watanabe K, Kimura Y, Hasegawa J, Nishino H. Triterpene acids from the leaves of *Perilla frutescens* and their anti-inflammatory and antitumor-promoting effects. *Biosci Biotechnol Biochem* 2004; **68**: 85-90
- 10 **Tokuda H**, Ohigashi H, Koshimizu K, Ito Y. Inhibitory effects of ursolic and oleanolic acid on skin tumor promotion by 12-O-tetradecanoylphorbol-13-acetate. *Cancer Lett* 1986; **33**: 279-285
- 11 **Subbaramaiah K**, Michaluart P, Sporn MB, Dannenberg AJ. Ursolic acid inhibits cyclooxygenase-2 transcription in human mammary epithelial cells. *Cancer Res* 2000; **60**: 2399-2404
- 12 **Mizushima Y**, Iida A, Ohta K, Sugawara F, Sakaguchi K. Novel triterpenoids inhibit both DNA polymerase and DNA topoisomerase. *Biochem J* 2000; **350 Pt 3**: 757-763
- 13 **Shishodia S**, Majumdar S, Banerjee S, Aggarwal BB. Ursolic acid inhibits nuclear factor-kappaB activation induced by carcinogenic agents through suppression of IkkappaBalpha kinase and p65 phosphorylation: correlation with down-regulation of cyclooxygenase 2, matrix metalloproteinase 9, and cyclin D1. *Cancer Res* 2003; **63**: 4375-4383
- 14 **Liu J**, Liu Y, Mao Q, Klaassen CD. The effects of 10 triterpenoid compounds on experimental liver injury in mice. *Fundam Appl Toxicol* 1994; **22**: 34-40
- 15 **Saraswat B**, Visen PK, Agarwal DP. Ursolic acid isolated from *Eucalyptus tereticornis* protects against ethanol toxicity in isolated rat hepatocytes. *Phytother Res* 2000; **14**: 163-166
- 16 **Ovesna Z**, Vachalkova A, Horvathova K, Tothova D. Pentacyclic triterpenoic acids: new chemoprotective compounds. Minireview. *Neoplasma* 2004; **51**: 327-333
- 17 **Tian Z**, Yang M, Huang F, Li K, Si J, Shi L, Chen S, Xiao P. Cytotoxicity of three cycloartane triterpenoids from *Cimicifuga dahurica*. *Cancer Lett* 2005; **226**: 65-75
- 18 **Miyase T**, Shiohara KI, Zhang DM, Ueno A. Araliasaponins I-XI, triterpene saponins from the roots of *Aralia decaisneana*. *Phytochemistry* 1996; **41**: 1411-1418
- 19 **Sambrook J**, Fritsch E F, Maniatis T, In Molecular cloning, A Laboratory Manual, 2nd ED.; Cold Spring Harbor Laboratory press: New York, 1989
- 20 **Chen WF**, Huang MH, Tzang CH, Yang M, Wong MS. Inhibitory actions of genistein in human breast cancer (MCF-7) cells. *Biochim Biophys Acta* 2003; **1638**: 187-196
- 21 **Livak KJ**, Schmittgen TD. Analysis of relative gene expression data using real-time quantitative PCR and the 2(-Delta Delta C(T)) Method. *Methods* 2001; **25**: 402-408
- 22 **Setzer WN**, Setzer MC. Plant-derived triterpenoids as potential antineoplastic agents. *Mini Rev Med Chem* 2003; **3**: 540-556
- 23 **Kujubu DA**, Fletcher BS, Varnum BC, Lim RW, Herschman HR. TIS10, a phorbol ester tumor promoter-inducible mRNA from Swiss 3T3 cells, encodes a novel prostaglandin synthase/cyclooxygenase homologue. *J Biol Chem* 1991; **266**: 12866-12872
- 24 **Jones DA**, Carlton DP, McIntyre TM, Zimmerman GA, Prescott SM. Molecular cloning of human prostaglandin endoperoxide synthase type II and demonstration of expression in response to cytokines. *J Biol Chem* 1993; **268**: 9049-9054
- 25 **DuBois RN**, Awad J, Morrow J, Roberts LJ 2nd, Bishop PR. Regulation of eicosanoid production and mitogenesis in rat intestinal epithelial cells by transforming growth factor-alpha and phorbol ester. *J Clin Invest* 1994; **93**: 493-498
- 26 **Eberhart CE**, Coffey RJ, Radhika A, Giardiello FM, Ferrenbach S, DuBois RN. Up-regulation of cyclooxygenase 2 gene expression in human colorectal adenomas and adenocarcinomas. *Gastroenterology* 1994; **107**: 1183-1188
- 27 **Tucker ON**, Dannenberg AJ, Yang EK, Zhang F, Teng L, Daly JM, Soslow RA, Masferrer JL, Woerner BM, Koki AT, Fahey TJ 3rd. Cyclooxygenase-2 expression is up-regulated in human pancreatic cancer. *Cancer Res* 1999; **59**: 987-990
- 28 **Buecher B**, Broquet A, Bouanchaud D, Heymann MF, Jany A, Denis MG, Bonnet C, Galmiche JP, Blottiere HM. Molecular mechanisms involved in the antiproliferative effect of two COX-2 inhibitors, nimesulide and NS-398, on colorectal cancer cell lines. *Dig Liver Dis* 2003; **35**: 557-565
- 29 **Detjen KM**, Welzel M, Wiedenmann B, Rosewicz S. Nonsteroidal anti-inflammatory drugs inhibit growth of human neuroendocrine tumor cells via G1 cell-cycle arrest. *Int J Cancer* 2003; **107**: 844-853
- 30 **Narayanan BA**, Condon MS, Bosland MC, Narayanan NK, Reddy BS. Suppression of N-methyl-N-nitrosourea/testosterone-induced rat prostate cancer growth by celecoxib: effects on cyclooxygenase-2, cell cycle regulation, and apoptosis mechanism(s). *Clin Cancer Res* 2003; **9**: 3503-3513
- 31 **Kim DK**, Baek JH, Kang CM, Yoo MA, Sung JW, Chung HY, Kim ND, Choi YH, Lee SH, Kim KW. Apoptotic activity of ursolic acid may correlate with the inhibition of initiation of DNA replication. *Int J Cancer* 2000; **87**: 629-636
- 32 **Yamagishi N**, Saito Y, Ishihara K, Hatayama T. Enhancement of oxidative stress-induced apoptosis by Hsp105alpha in mouse embryonal F9 cells. *Eur J Biochem* 2002; **269**: 4143-4151
- 33 **Yamagishi N**, Ishihara K, Saito Y, Hatayama T. Hsp105alpha enhances stress-induced apoptosis but not necrosis in mouse embryonal f9 cells. *J Biochem* 2002; **132**: 271-278
- 34 **Castelli C**, Rivoltini L, Rini F, Belli F, Testori A, Maio M, Mazzaferro V, Coppa J, Srivastava PK, Parmiani G. Heat shock proteins: biological functions and clinical application as personalized vaccines for human cancer. *Cancer Immunol Immunother* 2004; **53**: 227-233
- 35 **Wadhwa R**, Sugihara T, Yoshida A, Nomura H, Reddel RR, Simpson R, Maruta H, Kaul SC. Selective toxicity of MKT-077 to cancer cells is mediated by its binding to the hsp70 family protein mot-2 and reactivation of p53 function. *Cancer Res* 2000; **60**: 6818-6821